Journal of Power Sources 257 (2014) 45–51

Contents lists available at ScienceDirect

Journal of Power Sources

journal homepage: www.elsevier.com/locate/jpowsour

Reducing Pt use in the catalysts for formic acid electrooxidation via nanoengineered surface structure

Mengyin Liao [a], Yulu Wang [a], Guoqin Chen [a], Hua Zhou [a,*], Yunhua Li [a], Chuan-Jian Zhong [b], Bing H. Chen [a,*]

[a] Department of Chemical and Biochemical Engineering, College of Chemistry and Chemical Engineering, National Engineering Laboratory for Green Chemical Productions of Alcohols–Ethers–Esters, Xiamen University, Xiamen 361005, China
[b] Department of Chemistry, State University of New York at Binghamton, Binghamton, NY 13902, USA

HIGHLIGHTS

- A Pt decorated Pd/C with size (5–6 nm) was obtained by galvanic displacement.
- The catalyst with Pt:Pd molar ratio 1:250 has an unprecedented performance.
- The above catalyst has higher activity and stability than Pt/C and Pd/C.
- The controlled decorated structure can significantly reduce Pt use and thus cost.

ARTICLE INFO

Article history:
Received 15 November 2013
Received in revised form
31 December 2013
Accepted 22 January 2014
Available online 2 February 2014

Keywords:
Fuel cells
Platinum
Displacement reaction
Decorated catalyst
Formic acid electrooxidation
Ultralow Pt loading

ABSTRACT

The design of active and durable catalysts for formic acid (FA) electrooxidation requires controlling the amount of three neighboring platinum atoms in the surface of Pt-based catalysts. Such requirement is studied by preparing Pt decorated Pd/C (donated as Pt–Pd/C) with various Pt:Pd molar ratios via galvanic displacement making the amount of three neighboring Pt atoms in the surface of Pt–Pd/C tunable. The decorated nanostructures are confirmed by XPS, HS-LEIS, cyclic voltammetry and chronoamperometric measurements, demonstrating that Pt–Pd/C (the optimal molar ratio, Pt:Pd = 1:250) exhibits superior activity and durability than Pd/C and commercial Pt/C (J-M, 20%) catalysts for FA electrooxidation. The mass activity of Pt–Pd/C (Pt:Pd = 1:250) (3.91 A mg^{-1}) is about 98 and 6 times higher than that of commercial Pt/C (0.04 A mg^{-1}) and Pd/C (0.63 A mg^{-1}) at a given potential of 0.1 V vs SCE, respectively. The controlled synthesis of Pt–Pd/C lead to the formation of largely discontinuous Pd and Pt sites and inhibition of CO formation, exhibiting unprecedented electrocatalytic performance toward FA electrooxidation while the cost of the catalyst almost the same as Pd/C. These findings have profound implications to the design and nanoengineering of decorated surfaces of catalysts for FA electrooxidation.

1. Introduction

In view of the advantages over direct formic acid fuel cells (DFAFCs) including higher theoretical open circuit potential (1.45 V), lower fuel crossover, less positive oxidation potential and non-toxicity, the DFAFCs have been studied extensively and were considered as the great potential candidates for portable electronic devices [1–3]. It has been recognized that formic acid (FA) electrooxidation on metal surface contains a dual pathway mechanisms [4,5]: a direct pathway to CO_2 via a reactive intermediate; an indirect pathway via adsorbed CO (CO_{ad}) intermediate which is oxidized to CO_2 at high potentials. It is desirable for FA electrooxidation to go through "direct pathway" mechanism since this reaction pathway involves no significant CO poisoning. The catalysts commonly used for FA electrooxidation are either Pd-based [6–8] or Pt-based [9–11]. On pure Pt surface, CO poisoning due to the dehydration of FA on at least two or more contiguous Pt atoms (the ensemble) hinders the direct dehydrogenation oxidation of FA at lower overpotentials [12]. Nevertheless, the FA electrooxidation activity on monometallic Pd catalyst is still insufficient due to either the oxidation of Pd surface or the poisoning adsorption of some non-CO organic species [13,14]. Although the bimetallic Pt–Pd system has demonstrated as an effective alternative

* Corresponding authors. Tel.: +86 592 2185253; fax: +86 592 2184822.
E-mail addresses: cezhouh@xmu.edu.cn (H. Zhou), chenbh@xmu.edu.cn (B.H. Chen).

0378-7753/$ – see front matter © 2014 Elsevier B.V. All rights reserved.
http://dx.doi.org/10.1016/j.jpowsour.2014.01.103

approach for improving the electrocatalytic activity and stability of Pd catalysts in the FA oxidation reaction [15–17], it will be good to reduce the amount of Pt used in electrocatalyst to become more commercially acceptable.

Preparation of a decorated structure catalyst [18–22], in which the Pt is distributed on the surface of a substrate composed of a transition metal other than Pt, is doubtless an attractive approach as it offers the possibility of increasing Pt utilization and thus lowering Pt loading [23] in the catalysts. Among transition metals, Pd which is generally much cheaper than Pt is an option as it may provide better electrocatalytic activity. Wang and co-workers studied Pt decorated Pd/C catalysts with different atomic ratios of Pd to Pt and it was found that the catalytic activity towards FA electrooxidation was greatly enhanced owing to the reduction in three neighboring Pt atoms on the surface. When the atomic ratio of Pd to Pt atoms was 20:1, the catalytic activity reached a maximum value [24]. Kristian et al. prepared Pt submonolayer decorated Au nanocatalyst and it was found that the catalyst was superior to conventional Pt/C catalyst for FA electrooxidation. They attributed the enhanced performance to the reduction of three neighboring active sites of Pt and thus the depression of CO_{ad} formation [25]. Despite these prior achievements on Pt–Pd bimetallic composition whatever decorating or core–shell etc., a relatively high Pt loading is still required to be an efficient catalyst. Efforts are still putting on in terms of reducing the amount of Pt used while retain or even enhance the catalytic activity over the DFAFCs.

In this work, bimetallic nanoparticles with decorated Pt atoms and Pd substrate were designed and synthesized via a spontaneous displacement reaction ($Pd + PtCl_4^{2-} = Pt + PdCl_4^{2-}$), through which the amount of three neighboring Pt atoms in the surface of Pd-based catalysts could be controlled. A series of Pt decorated Pd (molar ratio, Pt:Pd = 1:100–1:300) nanoparticles dispersed on carbon black support had been initially synthesized and screened for FA electrooxidation. The decorated Pd atom layer, where Pt can be well dispersed, significantly reduces the presence of three neighboring Pt atoms, and thus efficiently suppresses CO formation. Moreover, both the decorated Pt atoms and the Pd substrate play the role of the active sites toward FA electrooxidation.

2. Experimental

2.1. Catalyst synthesis

The Pt–Pd/C catalysts were synthesized by a two-step method. Firstly, carbon supported Pd nanoparticles (metal loading: 20 wt %) were obtained using a reduction method [26,27]. In details, 100 mg carbon black (Vulcan® XC72R) was firstly dispersed into 10 mL ethanol under ultrasonication for 30 min. Then 20 mL ethanol solution containing 42 mg palladium chloride ($PdCl_2$) and 4.4 mg sodium citrate was added to the carbon black (Vulcan® XC72R) suspension and stirred sufficiently. Subsequently, 4 mL of ice-cold, freshly prepared 0.10 M $NaBH_4$ solution (prepared in NaOH solution with pH 12.0) was added to the above mixture rapidly. After that, the mixture was stirred for an additional 20 h at room temperature. Finally, the mixture was filtered, washed with deionized water. The carbon-supported Pd nanoparticles dried in a Vacuum oven at 70 °C for 4 h.

In the second step, 50 mg carbon supported Pd nanoparticles prepared above were submitted to another flask containing 20 mL deionized water and ultrasonicated for 30 min, 0.155 mg of K_2PtCl_4 (molar ratio, Pt:Pd = 1:250) aqueous solutions were added to the flask, then the mixture was stirred for 8 h at room temperature. Subsequently, the resulting powders were collected by filtration and then washed with deionized water until no chloride anion in the filtrate, and dried in air at 70 °C for 4 h. From these, the Pt–Pd/C catalysts were obtained.

2.2. Structural and compositional characterizations

A Technai F30 transmission electron microscope (TEM) operating at 300 keV was employed to evaluate the particle size and its distribution as well as morphology. The samples for TEM were dispersed in ethanol by ultra-sonication and then mounting the dispersed particles onto copper grids covered with a holey carbon film and then dried in air.

The X-ray photoelectron spectroscopy (XPS) measurement was performed on a PHI-Quantum 2000 spectrometer. Samples originally in powder form were pressed into a wafer to meet the analysis requirements. Binding energies were calibrated by referencing C1s at 284.6 eV as previous reference [28] recommended.

The HS-LEIS measurements were carried out on an IonTOF Qtac100 low-energy ion scattering analyzer. $^{20}Ne^{+}$ ions with a kinetic energy of 5 keV were applied at a low ion flux equal to 445 pA cm^{-2}. The scattering angle 145° was adopted in this work.

2.3. Electrochemical characterization

The electrochemical measurements of catalysts were carried out using an electrochemical workstation (CHI750d). A common three-electrode electrochemical cell was used for the measurements [29]. The counter and reference electrode were a platinum wire and a saturated calomel electrode (SCE) respectively. The working electrode was prepared by ultrasonicating 10 mg of the catalyst powder with 5 mL of aqueous solution containing 1 mL of isopropanol and 20 μL of a 0.25 wt % Nafion solution (diluted from a 5 wt % Nafion solution with ethanol, DuPont). 10 μL of the homogeneous catalyst ink was then dropcast onto a glassy carbon (GC) electrode and let it dry at room temperature. Cyclic voltammetry (CV) was conducted with a Pt flag counter electrode, a freshly polished GC working electrode (5 mm, Pine Instruments), and a saturated calomel electrode reference electrode. The potentials reported here are in reference to the saturated calomel electrode (SCE). All electrochemical experiments were recorded at room temperature. For assessing the electrocatalytic activity of the working electrode, cyclic voltammetry was obtained in 0.1 M $HClO_4$ + 0.5 M FA solution with a scan rate of 50 mV s^{-1}. For the durability test, the chronoamperometric experiments were carried out at 0.1 V for 3000 s in the same electrolyte.

3. Results and discussion

In this study, the fabrication of decorated structure catalyst using a two-step method as mentioned in experimental section 2.1 is firstly discussed. Firstly, the Pd nanoparticles were synthesized by a reduction method [26]. Secondly, some of the atoms in the outer layer of the Pd ($PdCl_4^{2-}/Pd$, $E^0 = 0.591$ V vs. SHE) were sacrificed to reduce $PtCl_4^{2-}$ ($PtCl_4^{2-}/Pt$, $E^0 = 0.775$ V vs. SHE) spontaneously. Using such procedures, there are both decorated Pt atoms and Pd substrate on carbon to form Pt–Pd/C catalysts as expecting.

3.1. Morphological and structural characteristics

It is difficult to observe the decorated structure of Pt–Pd/C directly by TEM, because the particles are too small and the Pt atoms of the surface are ultralow and generally well dispersed. Thus, Pt and Pd have almost the same crystal structure and characteristics in TEM images and difficult to distinguish. However, the TEM measurements give some important information for this catalyst. Fig. 1A,B shows TEM images of Pd/C and Pt–Pd/C (Pt:Pd = 1:250) catalysts. It can be seen that the metals are highly dispersed on the carbon supports and the average sizes being ca. 5.1 ± 0.8 nm and 5.2 ± 0.7 nm for Pd/C, Pt–Pd/C (Pt:Pd = 1:250)

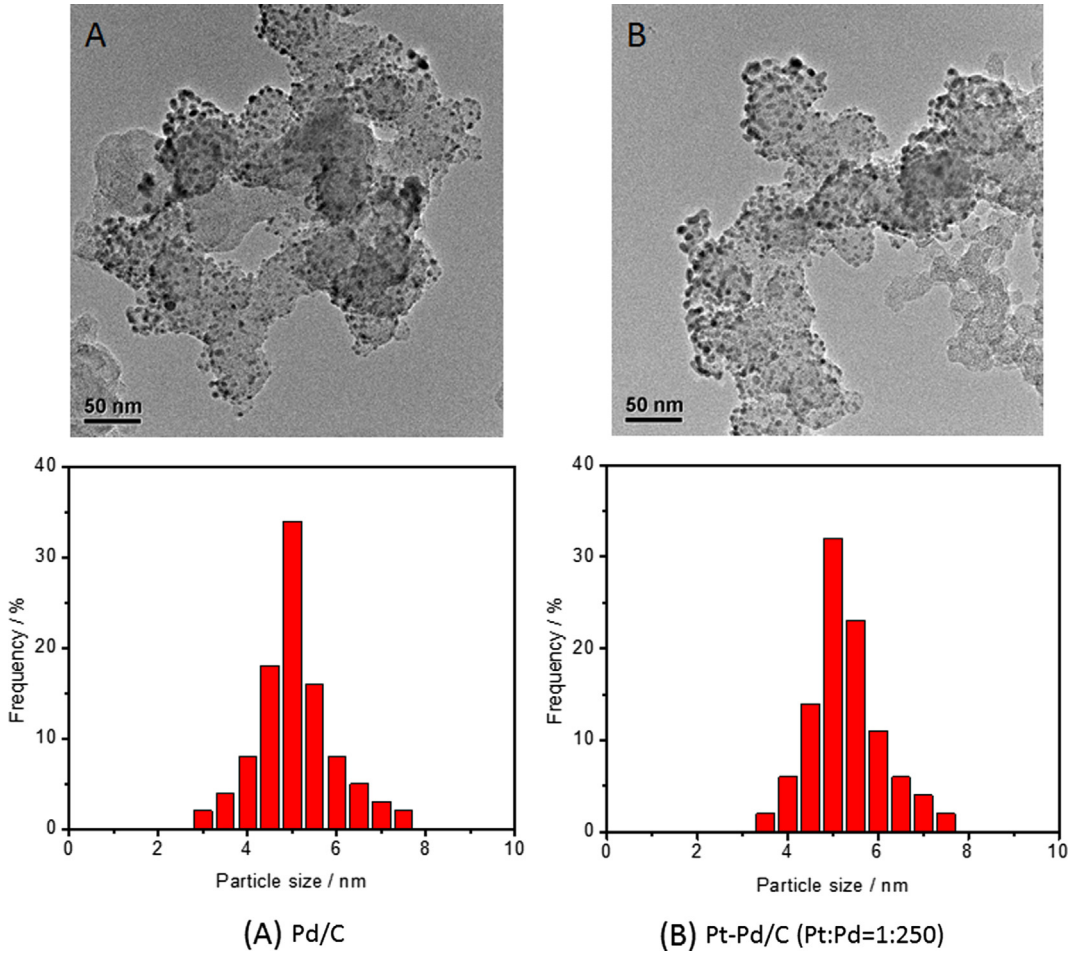

Fig. 1. TEM images and size distributions of Pd/C (A) and Pt–Pd/C (Pt:Pd = 1:250) (B) catalysts.

particles with a narrow size distributions. Armadi et al. showed the catalytic activity strongly depends on the size and size distribution of the metal particles, in addition to their dispersion on the supports [30]. Zhou et al. reported that the particle size effects on FA electrooxidation using carbon supported Pd nanoparticles with different sizes (2.7–9.0 nm), and pointed out that 5–7 nm Pd nanoparticles are most favorable for FA electrooxidation [31]. Therefore, Pt–Pd particles are within the optimal size range and Pt–Pd/C catalysts may be promoted to raise the specific activity. However, It is obvious that no significant differences between Pd/C and Pt–Pd/C (Pt:Pd = 1:250) catalysts are observed based on these TEM images.

XPS was employed to analyze the valence state and the surface composition of the carbon-supported metals. Fig. 2A shows the regional Pt4f spectra of commercial Pt/C and Pt–Pd/C (Pt:Pd = 1:250) catalysts. The Pt4f spectra shows a doublet containing a low energy band ($Pt4f_{7/2}$) and a high energy band ($Pt4f_{5/2}$) at 71.37 and 75 eV for commercial Pt/C and 71.62 and 75.12 eV for Pt–Pd/C (Pt:Pd = 1:250), respectively, the shifts of the peak positions can be observed for Pt4f, indicating the existence of metallic state Pt [32]. The decrease in the Pt binding energies for Pt–Pd/C (Pt:Pd = 1:250) relative to that of Pt/C suggests electronic interaction between Pt and Pd. Fig. 2B shows the regional Pd3d spectra of the Pd/C and Pt–Pd/C (Pt:Pd = 1:250) catalysts and no obvious shifts of the peak positions can be observed for Pd3d. Moreover, from Table 1, XPS spectra showed that the surface composition of Pt–Pd/C (Pt: Pd = 1:100), Pt–Pd/C (Pt: Pd = 1:150), Pt–Pd/C (Pt: Pd = 1:200), Pt–Pd/C (Pt: Pd = 1:250), Pt–Pd/C (Pt: Pd = 1:300) were found to be 1:84, 1:141, 1:180, 1:232, 1:293 (atomic ratio), respectively. It demonstrated that with the accession of the K_2PtCl_4 content increased, Pt replacement of Pd atoms on catalysts surface is really happened and increased. Furthermore, as can be seen in Table 1, the atomic fractions of Pt and Pd determined by ICP-MS in the nanocatalysts were in fact very close to the feeding ratio. No Pt was detected in the filtrated solution after the displacement reaction, indicating a completely spontaneous displacement of Pt and Pd in the synthesis process. It could be concluded that the bimetallic surface composition in the nanoparticles could be controlled by varying the feeding of the metal precursors used in the synthesis even though not exactly the same to the feeding.

To identify different chemical states of Pt, the XPS spectrum can be fitted by two pairs of overlapping Lorentzian curves. Fig. 2C,D shows the Pt4f spectrum of commercial Pt/C and Pt–Pd/C (Pt:Pd = 1:250) which could be deconvoluted into two components. Due to the chemisorptions of oxygen as inevitable explored in air, the spectra of both catalysts also appear the oxidation states of Pt (II) [33] and the slight differences in the binding states and the relative intensity of Pt (0) could be observed for both catalysts. Compared to commercial Pt/C, Pt–Pd/C (Pt:Pd = 1:250) has lower binding states and a larger portion of Pt (0). The relative areas indicate that metallic Pt (0) is the predominant species. Because no extraneous reducing agent was used, $PtCl_4^{2-}$ was believed to react exclusively with the Pd on Pd surface. Therefore, this result clearly

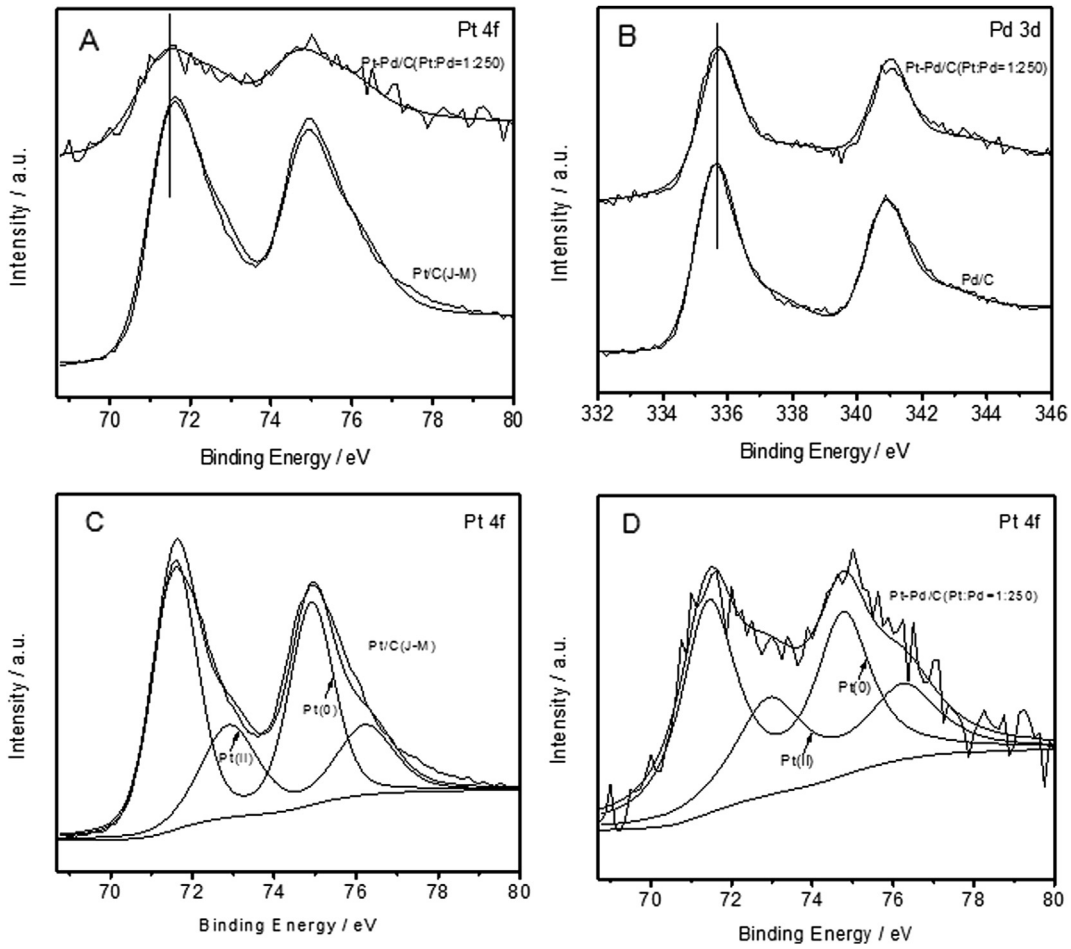

Fig. 2. Pt4f (A) XPS spectra of Pt–Pd/C (Pt:Pd = 1:250) and commercial Pt/C catalysts. Pd3d (B) XPS spectra of Pt–Pd/C (Pt:Pd = 1:250) and Pd/C catalysts. Pt4f XPS spectra of commercial Pt/C (C) and Pt–Pd/C (Pt:Pd = 1:250) (D) catalysts fitted by three pairs of overlapping Lorentzian curves.

shows a higher concentration of Pt on the particle surface in Pt–Pd/C, which supports the assessment that a decorated structure is formed for the Pt–Pd/C catalyst.

To further confirm the formation of the decorated structure in the catalyst prepared by the galvanic displacement technique, the high-sensitivity low-energy ion scattering (HS-LEIS) studies was implemented as the HS-LEIS is a surface-sensitive analytical technique used to characterize the chemical and structural makeup of materials and a powerful technique for understanding the atomic composition of the outmost atomic layer of the surface [34]. In HS-LEIS, the sample is bombarded with low-energy noble gas ions that are subsequently scattered by surface atoms. The backscattered ions are then energy analyzed in an electrostatic analyzer and their energies are related to the scattering elements by the laws of conservation of energy and momentum. The noble gas ions have high electron affinities and hence high neutralization probability on interaction with the surface. This restricts the information depth to one atomic layer as the ions penetrating the first layer have longer interaction time with the sample and thus will be effectively neutralized. Hence the signals coming from the multiple reflections can generally be neglected. Thus, the obtained spectra can be interpreted essentially as the mass spectra of surface atoms. The HS-LEIS spectra for the Pd/C, Pt–Pd/C (Pt:Pd = 1:100–1:300) are displayed in Fig. 3A. It is known that the Ne^+ ions can provide better sensitivities for heavier elements but not suitable for the measurement of lighter elements. Fig. 3B,C clearly shows that Pt and Pd co-exist on the outmost surface of the Pt–Pd/C (Pt:Pd = 1:100–1:300), and with decreasing Pt feeding for Pt–Pd/C (Pt:Pd = 1:100–1:300), the intensity of the Pd signal increased obviously and that of the Pt signal decreased snugly due to the weaker sensitivity for Pt compared with Pd and the ultralow Pt loading. Therefore, these HS-LEIS results provide further evidence for the formation of the decorated structure.

Table 1
Compositional for Pt–Pd/C (Pt:Pd = 1:100), Pt–Pd/C (Pt:Pd = 1:150), Pt–Pd/C (Pt:Pd = 1:200), Pt–Pd/C (Pt:Pd = 1:250), Pt–Pd/C (Pt:Pd = 1:300) catalysts.

Nanocatalysts	ICP-MS (Pt:Pd)	Surface compostion (Pt:Pd)
Pt–Pd/C(Pt:Pd = 1:100)	1:96	1:84
Pt–Pd/C(Pt:Pd = 1:150)	1:132	1:141
Pt–Pd/C(Pt:Pd = 1:200)	1:197	1:180
Pt–Pd/C(Pt:Pd = 1:250)	1:248	1:232
Pt–Pd/C(Pt:Pd = 1:300)	1:299	1:293

3.2. Electrochemical and electrocatalytic characteristics

Another evidence for the Pt decorating Pd comes from cyclic voltammetry (CV) as it can be regarded as a surface sensitive technique that only detects the electrochemical properties of surface atoms rather than bulk atoms [35]. Fig. 4 describes the cyclic voltammograms obtained in the N_2-purged electrolyte solution. The charges related to hydrogen adsorption/desorption (−0.2–0.075 V) and the oxidation/reduction of the metal (0.1–0.9 V) were

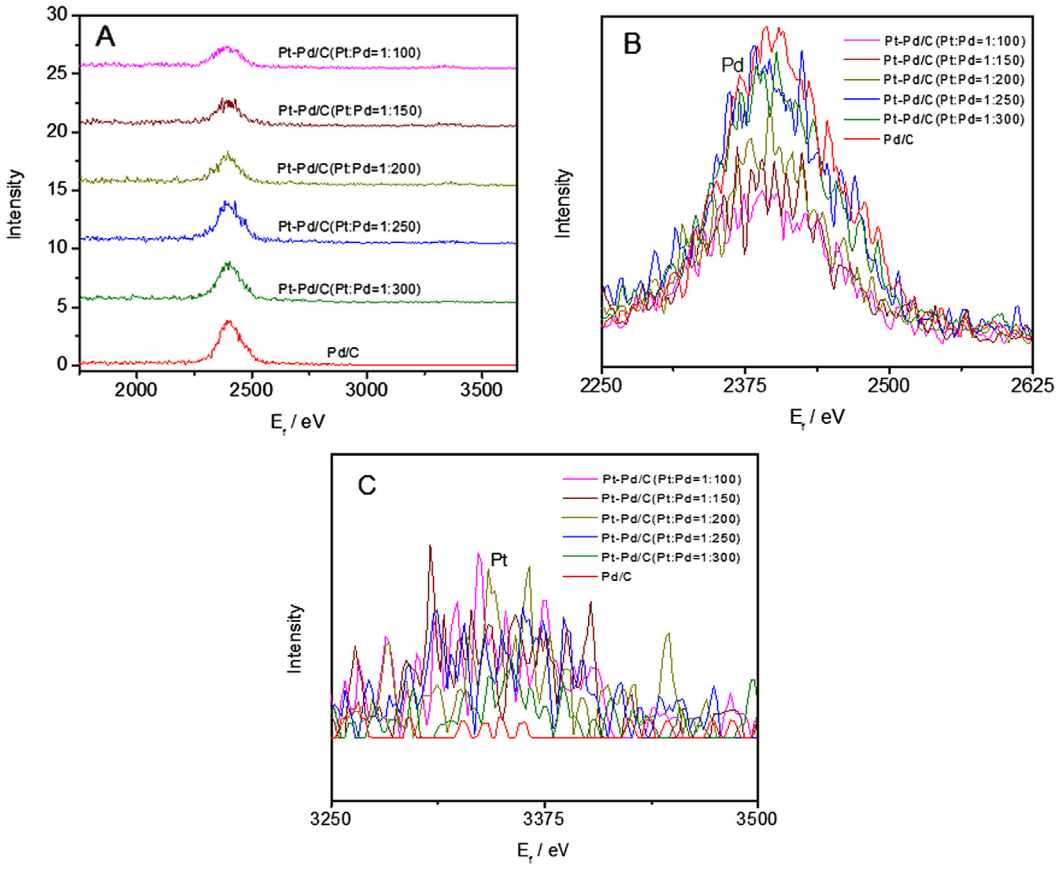

Fig. 3. (A) HS-LEIS spectra for Pd/C and Pt–Pd/C (Pt:Pd = 1:100), Pt–Pd/C (Pt:Pd = 1:150), Pt–Pd/C (Pt:Pd = 1:200), Pt–Pd/C (Pt:Pd = 1:250), Pt–Pd/C (Pt:Pd = 1:300) catalysts. (B) An expanded view of the Pd spectra of different catalysts. (C) An expanded view of the Pt spectra of different catalysts. 5 keV $^{20}Ne^{+}$.

observed in all the catalysts, while their positions and shapes are different to each other. Due to the hydrogen absorption being concomitant with hydrogen adsorption on the Pd surface, the Pd/C shows a distinct peak shape from that over Pt/C in the potential range −0.2–0.075 V. Although the Pt–Pd/C catalysts contained only a small amount of Pt, the peak shapes over these catalysts are more similar to that over Pt/C than Pd/C [36]. It implies that most of the Pd-based surfaces had already been covered partly by Pt atoms, and that an interaction occurred between the Pd substrate and the Pt in the surface. Furthermore, the electrochemical active area (ECA) of the Pt–Pd/C (Pt:Pd = 1:250) was high, up to 27.23 $m^2\ g^{-1}$, which was 5% higher than that of the Pd/C (25.93 $m^2\ g^{-1}$) [36,37]. This result revealed that the platinum was highly dispersed in the decorated structure catalyst.

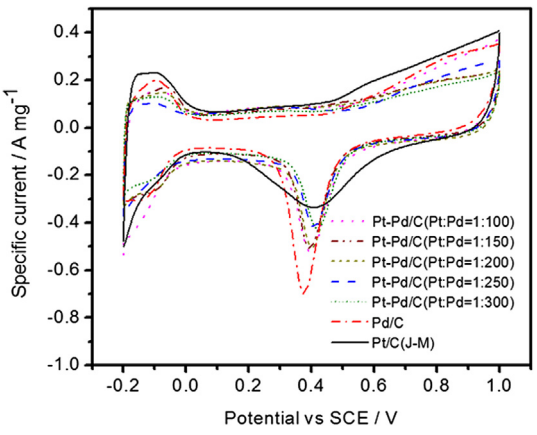

Fig. 4. Cyclic voltammograms for commercial Pt/C, Pd/C and Pt–Pd/C (Pt:Pd = 1:100), Pt–Pd/C (Pt:Pd = 1:150), Pt–Pd/C (Pt:Pd = 1:200), Pt–Pd/C (Pt:Pd = 1:250), Pt–Pd/C (Pt:Pd = 1:300) catalysts in N_2-saturated 0.1 M $HClO_4$ solution with a scan rate of 50 mV s^{-1}.

Fig. 5A shows a typical set of voltammograms for Pt–Pd/C catalysts with different amounts of decorated Pt atoms in N_2-saturated 0.1 M $HClO_4$ + 0.5 M FA solution with a scan rate of 50 mV s^{-1} at room temperature in the potential range of −0.25–0.8 V. For Pt/C, the small oxidation current at lower potentials in the forward scan was ascribed to surface CO poisoning resulting from self-dissociation of FA. By the contrast, in the backward scan with CO species removed at higher potentials, the FA oxidation current on Pt/C turned much higher before it decreased due to the regaining of surface CO. For Pt–Pd/C, the forward current of Pt–Pd/C catalysts are much lower than the backward current showing the similar characteristic features to Pt/C catalysts. There is a possibility that electronic effect of the bimetallic surface enhances the bond between Pt and CO_{ad}. Moreover, the peak potential decreases with the increase in Pt content in Fig. 5B, the peak potentials had small differences between Pt–Pd/C (Pt:Pd = 1:100–1:300) catalysts. The plot of peak current densities vs Pt:Pd molar ratio in nanoparticles shows a “volcano-like” for catalysts having 1:100–1:300 (Pt:Pd). When the atomic ratio of Pt and Pd atoms was 1:250, the catalytic activity was found to display a maximum. It should be emphasized that the peak potential of FA oxidation 0.134 V and the peak current density 4.06 A mg^{-1} are much more negative than the corresponding values obtained by other groups for other bimetallic nanostructures [38,39,40,41]. Cuesta et al. reported that at least three contiguous atoms are necessary for dehydration of FA to

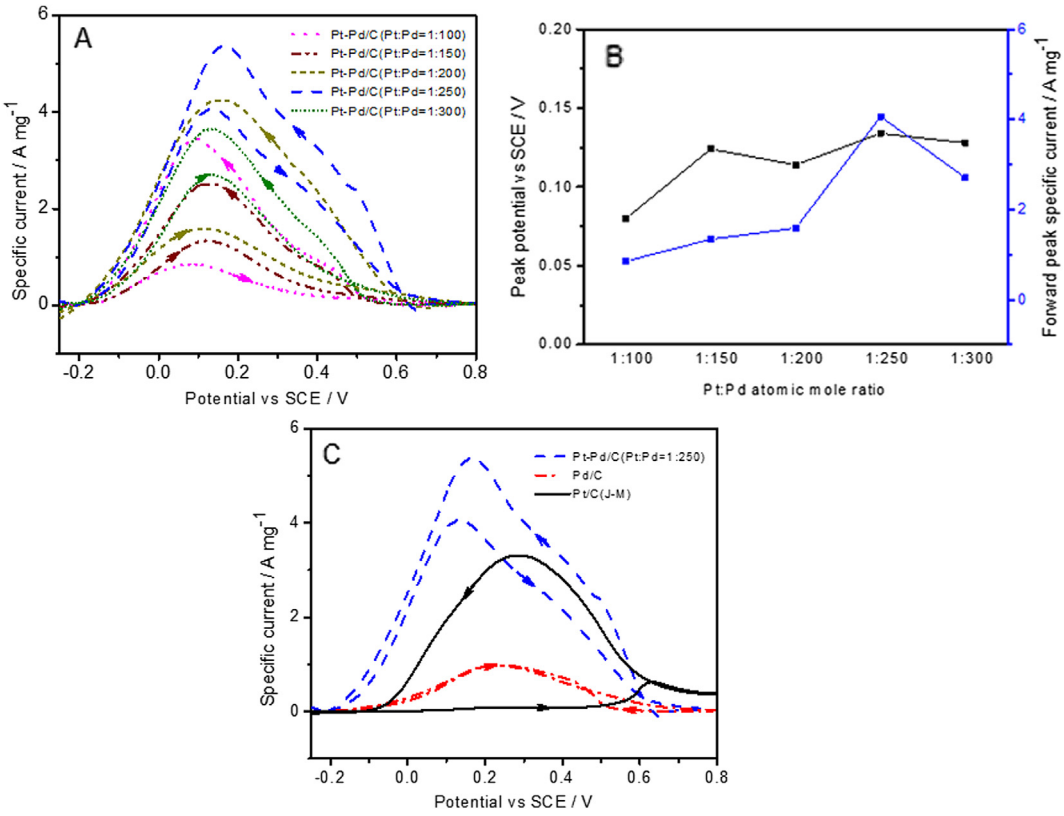

Fig. 5. (A) Cyclic voltammograms for Pt–Pd/C (Pt:Pd = 1:100), Pt–Pd/C (Pt:Pd = 1:150), Pt–Pd/C (Pt:Pd = 1:200), Pt–Pd/C (Pt:Pd = 1:250), Pt–Pd/C (Pt:Pd = 1:300) catalysts in N_2-saturated 0.1 M $HClO_4$ + 0.5 M FA solution with a scan rate of 50 mV s^{-1}; (B) Formic oxidation forward peak current density and peak potential vs Pt:Pd atomic ratio in Pt–Pd/C catalysts; (C) Cyclic voltammograms for commercial Pt/C, Pd/C and Pt–Pd/C (Pt:Pd = 1: 250) catalysts in N_2-saturated 0.1 M $HClO_4$ + 0.5 M FA solution with a scan rate of 50 mV s^{-1}.

adsorbed CO on Pt, with direct electrooxidation to CO_2 without passing through adsorbed CO being possible on a smaller atomic ensemble [42]. When a single FA molecule adsorbs and dissociates forming H_2O and an adsorbed CO residue, several neighboring Pt sites are required. Considering the dehydration of FA to form CO requires at least two neighboring Pt sites at the surface (the so-called ensemble effect [12,43]), decreasing the Pt atomic ratio in Pt–Pd/C obviously increases the chance for Pd atoms to surround single Pt atoms. It can be seen that the results are suggestive of a more important contribution from the distribution of Pt and Pd sites on the surface.

Fig. 5C illustrates another typical set of voltammograms for commercial Pt/C, Pd/C, Pt–Pd/C (Pt:Pd = 1:250) catalysts. The catalytic activity of the Pt–Pd/C (Pt:Pd = 1:250) catalyst (3.91 A mg^{-1}) is 6 times that of the Pd/C catalyst (0.63 A mg^{-1}), and 98 times that of the commercial Pt/C catalyst (0.78 A mg^{-1}), at a given potential of 0.1 V vs SCE. The improvement in the FA oxidation on the decorated structure can be due to the largely discontinuous Pd and Pt sites and the efficient removal of CO_{ads} formed in the dehydration path. Both Pt in the surface and Pd substrate are effective on the dehydration reaction. Moreover, from Fig. 3, with decreasing Pt feeding for Pt–Pd/C (Pt: Pd = 1:100–1:300), the intensity of the Pd signal increased and that of the Pt signal decreased gradually. This result can be explained by the deposition of Pt in the outmost Pd atom layer. This finding suggests that this optimal fraction of Pt and Pd atoms possibly led to an ordered surface arrangement of the metals responsible for the synergistic effect. On the other hand, the low activity for FA oxidation of Pt–Pd/C (Pt:Pd = 1:300) can be attributed to a small amount of Pt or almost no Pt.

Chronoamperometric experiments are carried out to observe the stability and possible poisoning of the catalysts under short time continuous operation. Fig. 6 shows such typical i–t plots with the current normalized to the initial current. For each catalyst, the decay in the FA oxidation is different. The Pt–Pd/C (Pt:Pd = 1:250) catalyst shows more stable than commercial Pt/C and Pd/C catalysts when the catalysts are compared under identical experimental conditions. It could be observed that the current at the commercial Pt/C, Pd/C, Pt–Pd/C (Pt:Pd = 1:250) catalysts at 1000 s are 0.08, 0.32, 0.54 A mg^{-1} precious metal, respectively. The above results demonstrate that the electrocatalytic stability of the Pt–Pd/C (Pt:Pd = 1:250) catalyst for FA oxidation is much higher than that of commercial Pt/C and Pd/C catalysts.

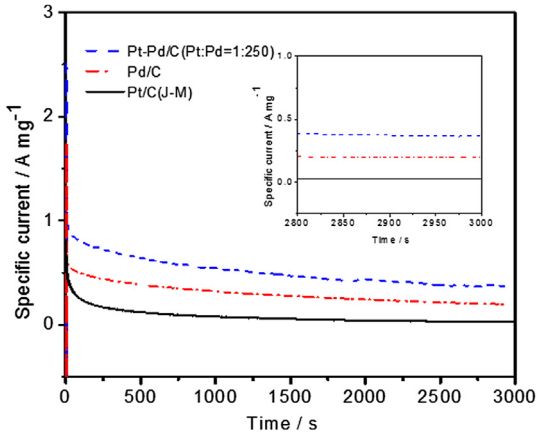

Fig. 6. Current–time curves recorded at 0.1 V (vs. SCE) for FA electrooxidation on commercial Pt/C, Pd/C and Pt–Pd/C (Pt:Pd = 1:250) catalysts in 0.1 M $HClO_4$ + 0.5 M FA solution.

4. Conclusions

In summary, the present results demonstrate that the use of Pt atoms decorated structure controlled Pd/C nanoparticles is an interesting strategy to enhance electrocatalytic activity. Surprisingly, ultralow Pt in the surface proved to be a distinct and powerful role in the Pd-based decorated structure catalyst. Pt decorated Pd/C catalyst with Pt:Pd (the optimal molar ratio, 1:250) has an unprecedented higher catalytic activity than commercial Pt/C and Pd/C catalysts, as a result of improved Pt utilization and Pt–Pd synergic effect. The work further proves that catalytic activity of Pt–Pd/C catalyst can indeed be improved through control the amount of three neighboring Pt atoms in the surface of Pd-based catalysts. Moreover, the findings in this work are important for the understanding of FA oxidation on a decorated surface, the development of advanced anode catalysts for direct formic acid fuel cells.

Acknowledgments

The authors would like to thank the Natural Science Foundation of China (Grant NSFC 20973140) and the Fundamental Research Funds for the Central Universities (Grant 201112G004) for financial supports.

References

[1] N.M. Aslam, M.S. Masdar, S.K. Kamarudin, W.R.W. Daud, APCBEE Procedia 3 (2012) 33–39.
[2] Y. Ohkubo, M. Shibata, S. Kageyama, S. Seino, T. Nakagawa, J. Kugai, H. Nitani, T. Yamamoto, J. Mater. Sci. 48 (2013) 2142–2150.
[3] A.N. Simonov, P.A. Simonov, V.N. Parmon, J. Power Sources 217 (2012) 291–295.
[4] S.G. Sun, J. Clavilier, A. Bewick, J. Electroanal. Chem. Interfacial Electrochem. 240 (1988) 147–159.
[5] M. Neurock, M. Janik, A. Wieckowski, Faraday Discuss. 140 (2009) 363–378.
[6] X. Yu, P.G. Pickup, J. Power Sources 182 (2008) 124–132.
[7] S. Hu, L. Scudiero, S. Ha, Electrochim. Acta 83 (2012) 354–358.
[8] D. Wu, Z. Zheng, S. Gao, M. Cao, R. Cao, Phys. Chem. Chem. Phys. 14 (2012) 8051–8057.
[9] B. Habibi, N. Delnavaz, Int. J. Hydrogen Energy 36 (2011) 9581–9590.
[10] I.-S. Park, K.-S. Lee, J.-H. Choi, H.-Y. Park, Y.-E. Sung, J. Phys. Chem. C 111 (2007) 19126–19133.
[11] W. Chen, J. Kim, L.-P. Xu, S. Sun, S. Chen, J. Phys. Chem. C 111 (2007) 13452–13459.
[12] S. Park, Y. Xie, M.J. Weaver, Langmuir 18 (2002) 5792–5798.
[13] X. Wang, Y. Tang, Y. Gao, T. Lu, J. Power Sources 175 (2008) 784–788.
[14] J.-Y. Wang, Y.-Y. Kang, H. Yang, W.-B. Cai, J. Phys. Chem. C 113 (2009) 8366–8372.
[15] E.A. Baranova, N. Miles, P.H.J. Mercier, Y. Le Page, B. Patarachao, Electrochim. Acta 55 (2010) 8182–8188.
[16] R. Larsen, S. Ha, J. Zakzeski, R.I. Masel, J. Power Sources 157 (2006) 78–84.
[17] P. Hong, F. Luo, S. Liao, J. Zeng, Int. J. Hydrogen Energy 36 (2011) 8518–8524.
[18] J. Zhang, F.H.B. Lima, M.H. Shao, K. Sasaki, J.X. Wang, J. Hanson, R.R. Adzic, J. Phys. Chem. B 109 (2005) 22701–22704.
[19] S. Papadimitriou, S. Armyanov, E. Valova, A. Hubin, O. Steenhaut, E. Pavlidou, G. Kokkinidis, S. Sotiropoulos, J. Phys. Chem. C 114 (2010) 5217–5223.
[20] A. Tegou, S. Papadimitriou, I. Mintsouli, S. Armyanov, E. Valova, G. Kokkinidis, S. Sotiropoulos, Catal. Today 170 (2011) 126–133.
[21] A. Tegou, S. Armyanov, E. Valova, O. Steenhaut, A. Hubin, G. Kokkinidis, S. Sotiropoulos, J. Electroanal. Chem. 634 (2009) 104–110.
[22] I. Mintsouli, J. Georgieva, S. Armyanov, E. Valova, G. Avdeev, A. Hubin, O. Steenhaut, J. Dille, D. Tsiplakides, S. Balomenou, S. Sotiropoulos, Appl. Catal. B Environ. 136–137 (2013) 160–167.
[23] H. Gao, S. Liao, J. Zeng, Y. Xie, D. Dang, Electrochim. Acta 56 (2011) 2024–2030.
[24] X.-M. Wang, M.-E. Wang, D.-D. Zhou, Y.-Y. Xia, Phys. Chem. Chem. Phys. 13 (2011) 13594–13597.
[25] N. Kristian, Y. Yan, X. Wang, Chem. Commun. 0 (2008) 353–355.
[26] Y.-C. Bai, W.-D. Zhang, C.-H. Chen, J.-Q. Zhang, J. Alloys Compd. 509 (2011) 1029–1034.
[27] G. Chen, M. Liao, B. Yu, Y. Li, D. Wang, G. You, C.-J. Zhong, B.H. Chen, Int. J. Hydrogen Energy 37 (2012) 9959–9966.
[28] Q. Li, Y. Zhang, G. Chen, J. Fan, H. Lan, Y. Yang, J. Catal. 273 (2010) 167–176.
[29] T. Maiyalagan, A.B.A. Nassr, T.O. Alaje, M. Bron, K. Scott, J. Power Sources 211 (2012) 147–153.
[30] T.S. Ahmadi, Z.L. Wang, T.C. Green, A. Henglein, M.A. El-Sayed, Science 272 (1996) 1924–1925.
[31] W. Zhou, J.Y. Lee, J. Phys. Chem. C 112 (2008) 3789–3793.
[32] D.J. Davis, G. Kyriakou, R.M. Lambert, J. Phys. Chem. B 110 (2006) 11958–11961.
[33] F. Liu, J.Y. Lee, W. Zhou, J. Phys. Chem. B 108 (2004) 17959–17963.
[34] H.H. Brongersma, M. Draxler, M. de Ridder, P. Bauer, Surf. Sci. Rep 62 (2007) 63–109.
[35] J. Luo, L. Wang, D. Mott, P.N. Njoki, Y. Lin, T. He, Z. Xu, B.N. Wanjana, I.I.S. Lim, C.-J. Zhong, Adv. Mater. 20 (2008) 4342–4347.
[36] Y.N. Wu, S.J. Liao, Y.L. Su, J.H. Zeng, D. Dang, J. Power Sources 195 (2010) 6459–6462.
[37] Y.-N. Wu, S.-J. Liao, Z.-X. Liang, L.-J. Yang, R.-F. Wang, J. Power Sources 194 (2009) 805–810.
[38] A.S. Bauskar, C.A. Rice, Electrochim. Acta 93 (2013) 152–157.
[39] J.D. Lović, M.D. Obradović, D.V. Tripković, K.D. Popović, V.M. Jovanović, S.L. Gojković, A.V. Tripkovi&cacute, Electrocatalysis 3 (2012) 346–352.
[40] Y. Chen, Y. Zhou, Y. Tang, T. Lu, J. Power Sources 195 (2010) 4129–4134.
[41] W. Wang, S. Ji, H. Wang, R. Wang, Fuel Cells 12 (2012) 1129–1133.
[42] A. Cuesta, M.a. Escudero, B. Lanova, H. Baltruschat, Langmuir 25 (2009) 6500–6507.
[43] S. Uhm, H.J. Lee, J. Lee, Phys. Chem. Chem. Phys. 11 (2009) 9326–9336.